materials

MDPI

Communication

Anti-Oxidation Agents to Prevent Dye Degradation in Organic-Based Host–Guest Systems Suitable for Luminescent Solar Concentrators

Francesca Villafiorita-Monteleone, Mariacecilia Pasini * and Chiara Botta *

Istituto di Scienze e Tecnologie Chimiche "Giulio Natta" (SCITEC), Consiglio Nazionale delle Ricerche (CNR), Sede Via A. Corti 12, 20133 Milano, Italy

* Correspondence: mariacecilia.pasini@scitec.cnr.it (M.P.); chiara.botta@scitec.cnr.it (C.B.)

Abstract: Luminescent solar concentrators (LSCs) have been extensively studied as they offer a practical solution to increase the efficiency of silicon-based photovoltaics (PVs). In this context, the use of natural and organic luminescent materials is desirable in order to obtain sustainable and environmentally friendly devices. Moreover, solution-processable organic host–guest systems based on Foerster Resonant Energy Transfer (FRET) processes offer the possibility to exploit a low-cost technique to obtain an efficient energy downshift from the UV–visible to red or deep red emissions in order to concentrate the radiation in the area of maximum efficiency of the PV device. Nevertheless, organic materials are subjected to photodegradation that reduces their optical properties when exposed to UV light and oxygen. In this work, we incorporated two different antioxidant molecules (i.e., octadecyl 3-(3,5-di-tert-butyl-4-hydroxyphenyl)propionate (Octa) and L-ascorbic acid (L-Asc)) in a three-dye host–guest system and studied the corresponding optical properties after prolonged irradiation times in air. It was found that the presence of the antioxidants, especially L-Asc, slowed the system's photodegradation down whilst at the same time retaining high emission efficiencies and without interfering with the cascade Resonant Energy Transfer processes among the dyes inserted in the nanochannels of the host.

Keywords: photodegradation; photostability; luminescent solar concentrators; host–guest systems; Foerster Resonant Energy Transfer; organic dyes; green energy; luminescent materials; antioxidants

check for updates

Citation: Villafiorita-Monteleone, F.; Pasini, M.; Botta, C. Anti-Oxidation Agents to Prevent Dye Degradation in Organic-Based Host–Guest Systems Suitable for Luminescent Solar Concentrators. *Materials* **2023**, *16*, 656. https://doi.org/10.3390/ma16020656

Academic Editor: Yongzhen Wu

Received: 21 November 2022
Revised: 2 January 2023
Accepted: 5 January 2023
Published: 10 January 2023

Copyright: © 2023 by the authors. Licensee MDPI, Basel, Switzerland. This article is an open access article distributed under the terms and conditions of the Creative Commons Attribution (CC BY) license (https://creativecommons.org/licenses/by/4.0/).

1. Introduction

As the human population grows, the development of sustainable, affordable and environmentally friendly energy production is crucial. Renewable energy, especially solar photovoltaic (PV) technology, provides the possibility for solving resource and environmental issues with the advantage of zero CO_2 emissions [1–3]. Unfortunately, the cost of generating electricity from silicon solar cells remains high [4], not to mention that the waste generated during their production and after their end-of-life hurts the environment and cannot be ignored [5].

Luminescent solar concentrators (LSCs) are a widely studied and viable solution to the fabrication of sustainable and cheap PV systems characterized by high transparency, light weight, limited costs, synthetic versatility, high absorption coefficients and an ability to capture both incident and diffuse light [6–8]. Moreover, they can be fully integrated into architectural elements and become part of a building's skin unit [9–11].

Basically, an LSC is a coating of luminescent materials consisting of dopants dispersed in an optically transparent host material (i.e., polymer matrices or glass substrates) acting as optical waveguide, in which the luminescent materials absorb both direct and indirect sunlight and then emit downshifted photons through a photoluminescence (PL) process (usually fluorescence) [6,12]. A large portion of the emitted light is concentrated via Total Internal Reflection (TIR) to the edges of the LSC, where a strip of PV cells may be attached,

to collect the emitted light and convert it to an electrical current [13]. In this way, the possibility of concentrating the light radiation through Energy Transfer (ET) processes in the area of maximum efficiency of the device allows the minimizing of the size of the solar cells, with a consequent benefit in terms of production costs and environmental impact.

Up to now, various luminescent materials have been used as dopants, such as organic dyes [14–17], metal clusters [18,19], inorganic quantum dots [20–24], perovskites nanocrystals [25,26] and, more recently, carbon dots [27,28].

Despite the simple design and much needed applications, the widespread use of LSCs is still challenging, predominantly due to the photodegradation of both matrices and luminophores [6,29–32] and the reduced device efficiency, which in turn is linked to various light-loss processes [6,33–35].

In this context, potential approaches to minimize the absorption losses include the use of fluorescent dyes with a tunable Stokes shift [8,16,36,37], the use of luminophores with Aggregation-Induced Emission (AIE) properties [38,39] and, mostly, the use of organic or hybrid host–guest systems and the exploitation of Foerster Resonant Energy Transfer (FRET) processes, since they allow a significant improvement in the light-absorption efficiency while, at the same time, reducing reabsorption losses [40–45].

At the same time, to reduce the undesirable degradation effects of solar radiation on the luminophores, several approaches have been considered, ranging from the deliberate structural modification of dyes to the use of protective agents of various kinds. A variety of additives have been commercially developed, which can be used either before, during or after the incorporation of the dye in the device. Such additives may protect the dye, the matrix or, ideally, both [46,47].

In this work, we present a study on the photostability of deoxycholic acid (DCA)-based host–guest materials containing three linear dyes (Figure 1a) (diphenylhexatriene (DPH) emitting in the blue (Figure 1b), 4,7-di(2-thienyl)-benzo[1–3]thiadiazole (DBT) emitting in the green (Figure 1c), and 4,7-bis(5′-hexyl-2,2′-bithienyl-5-yl)-2,1,3-benzothiadiazole (DBTT) emitting in the red (Figure 1d)) for the development of photostable LSCs.

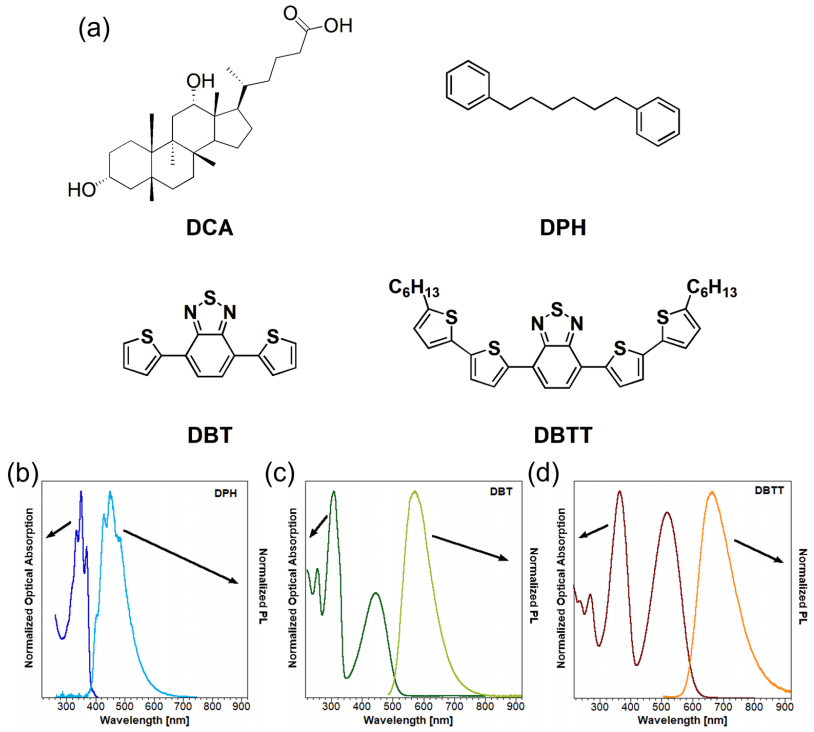

Figure 1. (**a**) Chemical structures of DCA, DPH, DBT and DBTT. Absorption and photoluminescence spectra of (**b**) DPH in MeOH and (**c**) DBT and (**d**) DBTT in THF, with excitation wavelengths at 360 nm, 420 nm and 500 nm, respectively.

These systems have previously been demonstrated to be able to shift the near UV and visible light to the deep red with a very high efficiency, thanks to controlled FRET processes among the dyes inserted in the nanochannels characteristic of a DCA organic host [42,48]. Here, we exposed thin films of these materials to prolonged irradiation in order to test their performances in LSC devices.

To avoid the photodegradation of the systems, we added some antioxidant molecules and studied the effect of their presence on the materials' optical properties.

2. Materials and Methods

2.1. Materials

Deoxycholic acid (DCA), 1,6-diphenyl-1,3,5-hexatriene (DPH), octadecyl 3-(3,5-di-tert-butyl-4-hydroxyphenyl)propionate (Octa) and L-ascorbic acid (L-Asc) were purchased from Sigma Aldrich and used without further purification. 4,7-Di(2-thienyl)-benzo[1–3]thiadiazole (DBT) and 4,7-bis-(5′-hexyl-2,2′-bithienyl-5-yl)-2,1,3-benzothiadiazole (DBTT) were synthesized as reported elsewhere [49–51]. All solvents were of analytical grade.

The DCA mother solution was prepared with a concentration of about 10^{-2} M, and antioxidant and dye mother solutions were prepared with a concentration of about 7×10^{-3} M in THF. Reference samples were prepared by mixing DCA and dye mother solutions in order to prepare co-inclusions with the following ratios: DCA:DPH=3:1 and DPH:DBT:DBTT = 96.9:2.9:0.2. Antioxidant mother solutions with a concentration of about 2×10^{-3} M in THF were mixed with co-inclusion mother solutions in order to have DBT:antioxidant concentrations of 90 and 10, 80 and 20 and 95 and 5 wt.%.

Films of DCA inclusion compounds with and without antioxidants were obtained by spin-coating the corresponding solutions at 500 rpm for 60 s on 2×2 cm^2 quartz substrates. The resulting films had a thickness of about 150–200 nm.

2.2. Optical Characterization

PL measurements on solid state samples in air at room temperature were obtained with a SPEX 270 M monochromator equipped with a N_2-cooled charge-coupled device excited with a monochromated Xe lamp. The spectra were corrected for the instrument response. PL quantum yields (QYs) (The Photoluminescence Quantum Yield of a molecule or material is defined as the number of photons emitted as a fraction of the number of photons absorbed [52]) of solid state materials were obtained by using a homemade integrating sphere and by correcting the spectra for the background of the exciting lamp according to [48].

For accelerated photodegradation experiments, all samples were subjected to continuous illumination in air by means of a UV-lamp (Hamamatsu L9566 series) with a 300–400 nm band-pass excitation filter at a 30 mm distance, where the lamp intensity was about 410 mW/cm^2 (Scheme 1).

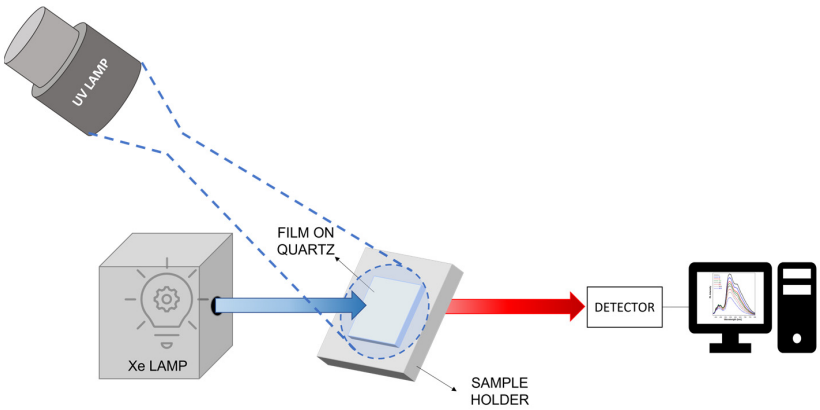

Scheme 1. Scheme of the optical setup used for the photodegradation experiments and fluorescence spectra collection.

Fluorescence spectra were collected after each period of exposure (0, 5, 10, 30, 45, 60, 80, 90, 105, 120, 180, 300, 480, 960, 1800, 3600 s) with the above-mentioned apparatus. The photodegradation was followed by monitoring the decrease in the overall emission and/or in each dye emission band (i.e., in the 400–475 nm range for DPH, in the 475–585 nm range for DBT and in the 585–750 nm range for DBTT). The decrease in the emission intensity for both the DCA-DPH:DBT and the DCA-DPH:DBT:DBTT samples was analyzed, with a bi-exponential fit with and without antioxidants.

3. Results and Discussion

As previously reported, thin films of organic host–guest systems based on the use of DCA, obtained from bovine bile, as the host involve the use of sustainable and natural components and can be obtained with low-cost self-assembly technology [42,48].

These materials can be used to obtain films with a three-dye system able to efficiently downshift the near-UV-visible light to deep red thanks to controlled FRET processes, in order to develop LSCs with reduced energy consumption [42]. Moreover, to obtain such highly efficient host–guest systems, it is sufficient to use a small amount of DBT with respect to DPH to shift the system's emissions from blue to green, and thus to use an even smaller quantity of DBTT with respect to DBT to shift the emission from green to red, as demonstrated elsewhere [42].

As shown in Figure 1b–d, the three dyes were characterized by optical properties ideal for a cascade FRET process to shift the energy from the near-UV (DPH absorption) region to the green (DBT emission) region and, finally, to the deep red (DBTT emission) region. This system worked because the absorption of each acceptor overlapped with the emission of each donor, and the relative Foerster radii led to an efficient funneling from the UV region to the deep red region through a multi-step FRET process (DPH → DPH, DPH → DBT, DPH → DBTT and DBT → DBTT) [42].

Indeed, the thin films of co-inclusions of DPH, DBT and DBTT in DCA showed emissions from all chromophores when the DPH was excited (Figure 2). It was, in fact, possible to recognize the emission bands of each dye: DPH presented an emission peak in the 400–475 nm range, DBT in the 475–585 nm range and DBTT in the 585–750 nm range.

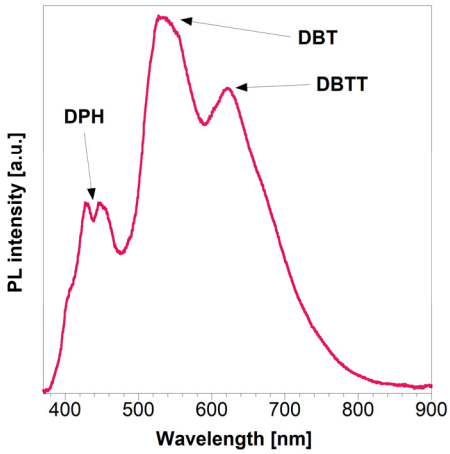

Figure 2. PL emission spectrum of a DCA-DPH:DBT:DBTT spin-coated film without any additives, with DPH:DBT:DBTT molar ratios of 96.9:2.9:0.2. The sample was excited at 360 nm.

One major drawback against the wide diffusion of organic systems such as the one just described is the photostability of the materials that unfortunately are subjected to degradation when exposed to UV light and oxygen. The inclusion of organic dyes into a DCA host is expected to protect the dyes from photodegradation, since the host reduces their exposure to oxygen [42,48]. Thus, to assess their use in LSC devices, we performed an accelerated aging test on host–guest thin films by exposing them to prolonged irradiation in air. Aging the films with a UV lamp in air induced an emission quenching, as shown in

Figure 3, where the emission spectra of the bare DCA-DPH:DBT:DBTT films are compared for increasing irradiation times.

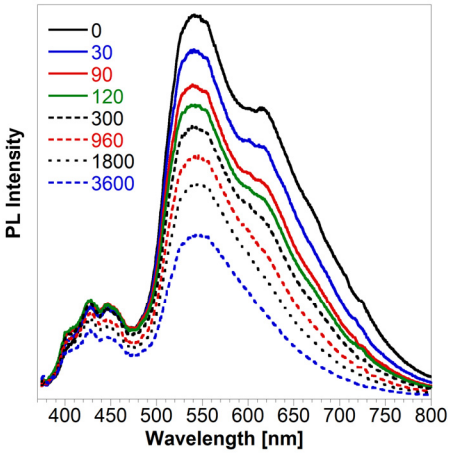

Figure 3. PL emission spectra of the DCA-DPH:DBT:DBTT films without any additives with different times of UV light irradiation (from 0 to 3600 s).

It is possible to notice an evident quenching in the overall fluorescence intensity with increasing light exposure times, even though some differences can be highlighted. Specifically, a sharp emission decrease was observed for the peaks associated with DBT and DBTT (in the 475–585 nm and 585–750 nm ranges, respectively (Figure 2)) in the host–guest system, whereas a slower and less pronounced reduction in the PL intensity was detected for the peak associated with DPH (in the 400–475 nm range, Figure 2). This behavior is better highlighted in Figure 4, where the changes in the emission intensities are reported as the ratio between the emission intensity measured after a specific time interval (I) and the initial emission intensity (I_0).

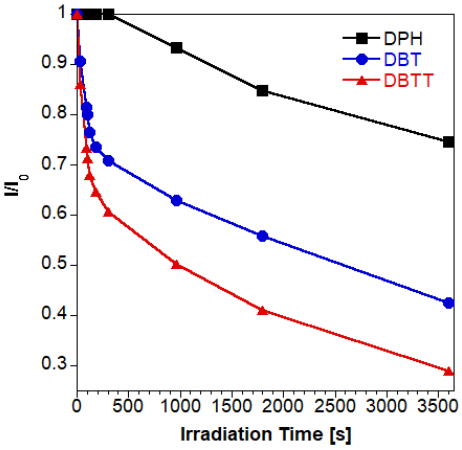

Figure 4. PL emission intensity ratios of the DPH (square), DBT (circle) and DBTT (triangle) components of the inclusion compounds in DCA, without any additives, as a function of UV light exposition.

These different quenching behaviors could be due to the differences in the chemical structures of the chromophores. In fact, thiophene-based materials are more easily subjected to photooxidation, as previously reported [53–56]. Indeed, the presence of thiophene groups in both DBT and DBTT leads to a larger number of sites ideal for oxidative reactions.

To assess the role of the antioxidants on the overall stability, we started with DCA-DPH:DBT co-inclusion compounds and evaluated the effect of different additive concentrations (5 wt.%, 10 wt.% and 20 wt.% with respect to the DBT concentration). We chose two different antioxidant molecules: octadecyl 3-(3,5-di-tert-butyl-4-hydroxyphenyl)propionate (Octa) and L-ascorbic acid (L-Asc) (Scheme 2). The former is a synthetic antioxidant, largely

used in plastics and food packaging [57] and is large enough to act as stopcock by inserting its long alkyl chain inside the host channel and blocking the entrance thanks to the bulky benzene derivative [58,59]. The latter is the L-enantiomer of ascorbic acid, a natural water-soluble vitamin, small enough to enter the DCA nano-channels and suitable for green chemistry [60].

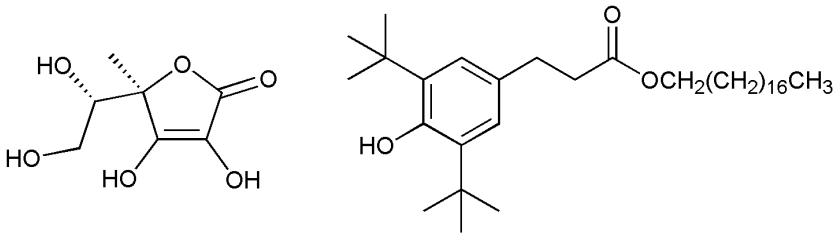

L-Asc **OCTA**

Scheme 2. Chemical structures of L-Asc (**left**) and Octa (**right**).

We exposed the host–guest systems in air to UV light for increasing time intervals and monitored the photodegradation of the organic components by means of fluorescence spectroscopy.

As shown in Figure 5, after different irradiation times, almost all the additive concentrations led to an improvement in the resistance to photodegradation when compared with the bare sample. According to the experiment, the best results were achieved with a concentration of 10 wt.% for both antioxidants: higher antioxidants concentrations had a negative or no effect because of the changes in the FRET process.

Table 1. Parameters of bi-exponential fits of the photodegradation aging tests and corresponding decay times for DCA-DPH:DBT samples with and without 5 wt.%, 10 wt.% and 20 wt.% of antioxidants ($t_{av}=\frac{\sum_{n=1}^{2} A_n t_n}{\sum_{n=1}^{2} A_n}$).

	t_1 (min)	A_1	t_2 (min)	A_2	Adj. R-Square	t_{av} (h)
DCA-DPH:DBT	0.926	0.23	476.2	0.77	0.87195	6.121
5 wt.% Octa	1.191	0.18	505.1	0.82	0.98173	6.868
10 wt.% Octa	1.191	0.18	537.6	0.82	0.97987	7.368
20 wt.% Octa	1.235	0.25	282.5	0.75	0.99558	3.533
5% L-Asc	1.235	0.185	366.3	0.815	0.99370	4.979
10% L-Asc	1.587	0.10	555.6	0.90	0.98965	8.345
20% L-Asc	1.282	0.11	656.2	0.89	0.97563	9.734

The comparison of the decay times (Table 1), obtained as averages of the bi-exponential fits, confirmed the choice of using 10 wt.% of additive as the best-performing anti-oxidant concentration.

Thus, for the complete systems characterized by the co-inclusion of the three dyes, we considered the addition of 10 wt.% of L-Asc or Octa. Figure 6 shows the degradation of all the samples' emissions as a function of different UV light irradiation times. In addition, for the complete system, the presence of L-Asc seemed to reduce the photodegradation with respect to both the bare system and the sample with Octa. In fact, after 1h of irradiation in accelerated photodegradation conditions, the intensity was still 85%. Moreover, as reported in Table 2, the lifetime increased from 5.9 h to 12.1 h with the addition of 10 wt.% L-Asc to the DCA matrix. This result might be due to the fact that L-Asc is a small molecule that penetrates the DCA nanochannels and performs its antioxidant function within close proximity of the dyes [60].

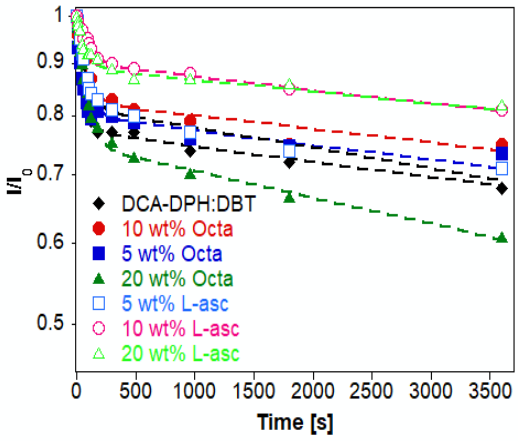

Figure 5. PL emission intensity ratios of bare DCA-DPH:DBT (full black square) and DCA-DPH:DBT with 5 wt.% (full blue square), 10 wt.% (full red circle) and 20 wt.% (full green triangle) of Octa and with 5 wt.% (empty black diamond), 10 wt.% (solid pink triangle) and 20% (empty square) of L-Asc as a function of UV light exposition. Dotted lines are bi-exponential fits (see Table 1).

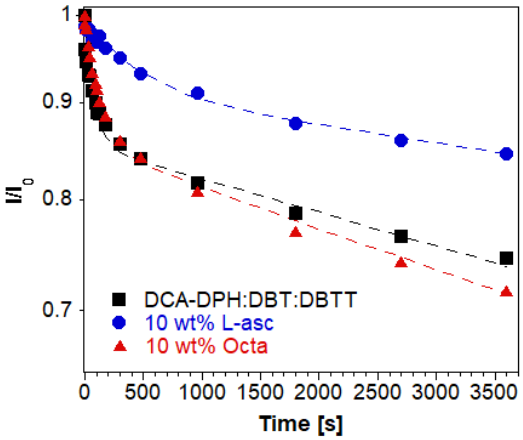

Figure 6. PL emission intensity ratios of bare DCA-DPH:DBT:DBTT (full black square) and DCA-DPH:DBT:DBTT with 10 wt.% L-Asc (full blue circle) and 10 wt.% Octa (full red square) as a function of UV light exposition time. Dotted lines are bi-exponential fits (see Table 2).

Table 2. Parameters of bi-exponential fits and corresponding decay times of the photodegradation aging tests for DCA-DPH:DBT:DBTT samples with and without 10 wt.% antioxidants, prepared in air or in an inert atmosphere ($t_{av}=\frac{\sum_{n=1}^{2} A_n t_n}{\sum_{n=1}^{2} A_n}$).

	t_1 (min)	A_1	t_2 (min)	A_2	Adj. R-Square	t_{av} (h)
DCA-DPH:DBT:DBTT	1.389	0.14	411.5	0.86	0.98145	5.926
10 wt.% Octa	2.083	0.15	340.1	0.85	0.9907	4.826
10 wt.% L-Asc	7.576	0.09	793.7	0.91	0.99124	12.10
DCA-DPH:DBT:DBTT (inert atmosphere)	1.235	0.07	957.9	0.94	0.99223	14.93

To further assess the role of the antioxidant molecules added to the co-inclusion compounds as means for improving the photostability, we compared the additive-containing systems to bare co-inclusions prepared in an oxygen-free environment and then subjected them to UV irradiation in air. Figure 7 shows the PL emission intensity ratios of the DCA-DPH:DBT:DBTT samples prepared in air or in an inert atmosphere and of the systems containing L-Asc or Octa prepared in air.

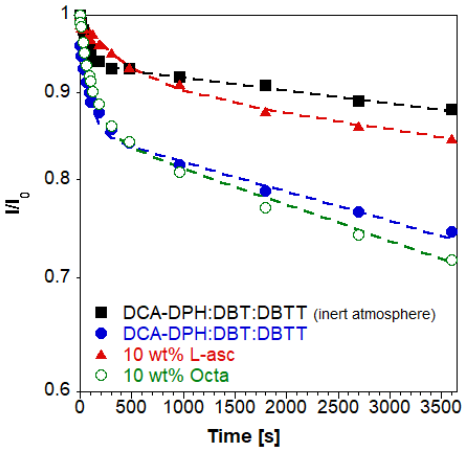

Figure 7. PL emission intensity ratios of bare DCA-DPH:DBT:DBTT prepared in inert atmosphere (full square) and in air (full circle) and DCA-DPH:DBT:DBTT with 10 wt.% L-Asc (full triangle) and 10 wt.% Octa (empty square), both prepared in air, as a function of UV light exposition. Dotted lines are bi-exponential fits (see Table 2).

As shown in the following plot and in Table 2, the presence of L-Asc led to an initial lower photodegradation when compared to the bare samples prepared in the absence of oxygen, showing an emission loss of a maximum of 25% despite being prepared in air. As stated above, this might be due to the small dimensions of this particular antioxidant that easily penetrates inside the DCA nanochannels and performs its role in eliminating reactive oxygen species directly in situ [60].

Finally, we performed a last aging test, exposing all the samples to air and natural light for one week and measuring their absolute PL QYs before and after UV exposure. Table 3 shows the values for the bare samples prepared either in the absence of oxygen or in air and for the additive-containing systems prepared in air, before and after the aging experiments. Once again, the samples prepared with 10 wt.% of L-Asc showed the best results, with no emission losses whatsoever. This result demonstrates that the inclusion of L-Asc as an anti-oxidation agent in DCA films containing three organic dyes reduced the emission-quenching processes typical of organic materials, allowing the preparation of thin films from solutions in air with simple and low-cost techniques.

Table 3. PL QY values of as-prepared samples (either prepared in an oxygen-free atmosphere or in air) and after one week of air and light exposure, with and without antioxidants.

	Inert Atmosphere	1 Week Old	Air	1 Week Old
DCA-DPH:DBT:DBTT	1	0.83	0.97	0.81
10 wt.% L-Asc	-	-	1	1
10 wt.% Octa	-	-	0.83	0.73

4. Conclusions

We studied the possibility of increasing the photostability of organic host–guest systems suitable for LSC applications by comparing two different antioxidant molecules: octadecyl 3-(3,5-di-tert-butyl-4-hydroxyphenyl)propionate (Octa), a synthetic antioxidant, largely used in plastics and food, and L-ascorbic acid (L-Asc), a natural water-soluble vitamin found in fruit and vegetables. In particular, the use of L-Asc enables the obtaining of natural and environmentally friendly compounds and the improvement of the system's photostability without recurring to encapsulation or preparation procedures involving an inert atmosphere, thus following a very simple and low-cost technique (i.e., deposition in air of solutions containing the different compounds) for the production of organic thin films compatible with the realization of low-cost LSCs.

Although this work is in its infancy, these values and the stability of the presented systems as optically active materials are a promising starting point for the development of sustainable and stable LSCs.

Author Contributions: Conceptualization, F.V.-M., M.P. and C.B.; data analysis, F.V.-M.; writing—original draft preparation, F.V.-M.; writing—review and editing, F.V.-M., M.P. and C.B.; supervision, M.P. and C.B. All authors have read and agreed to the published version of the manuscript.

Funding: This research was partially funded by Fondazione Cariplo, through the project "Functional carbon dots for ENhancing tomato production In a Circular Economy scheme (FENICE)", grant number 2021-0626.

Institutional Review Board Statement: This study did not require any ethical approval.

Informed Consent Statement: Not applicable.

Data Availability Statement: The data presented in this study are available within the article and in ref. [42].

Conflicts of Interest: The authors declare no conflict of interest.

References

1. Gürtürk, M. Economic Feasibility of Solar Power Plants Based on PV Module with Levelized Cost Analysis. *Energy* **2019**, *171*, 866–878. [CrossRef]
2. Alaaeddin, M.H.; Sapuan, S.M.; Zuhri, M.Y.M.; Zainudin, E.S.; Al-Oqla, F.M. Photovoltaic Applications: Status and Manufacturing Prospects. *Renew. Sustain. Energy Rev.* **2019**, *102*, 318–332. [CrossRef]
3. Almosni, S.; Delamarre, A.; Jehl, Z.; Suchet, D.; Cojocaru, L.; Giteau, M.; Behaghel, B.; Julian, A.; Ibrahim, C.; Tatry, L.; et al. Material Challenges for Solar Cells in the Twenty-First Century: Directions in Emerging Technologies. *Sci. Technol. Adv. Mater.* **2018**, *19*, 336–369. [CrossRef] [PubMed]
4. Cui, Y.; Lieber, C.M. Functional Nanoscale Electronic Devices Assembled Using Silicon Nanowire Building Blocks. *Science* **2001**, *291*, 851–853. [CrossRef]
5. Qi, L.; Zhang, Y. Effects of Solar Photovoltaic Technology on the Environment in China. *Environ. Sci. Pollut. Res.* **2017**, *24*, 22133–22142. [CrossRef]
6. Debije, M.G.; Verbunt, P.P.C. Thirty Years of Luminescent Solar Concentrator Research: Solar Energy for the Built Environment. *Adv. Energy Mater.* **2012**, *2*, 12–35. [CrossRef]
7. Papakonstantinou, I.; Portnoi, M.; Debije, M.G. The Hidden Potential of Luminescent Solar Concentrators. *Adv. Energy Mater.* **2021**, *11*, 2002883. [CrossRef]
8. Mazzaro, R.; Vomiero, A. The Renaissance of Luminescent Solar Concentrators: The Role of Inorganic Nanomaterials. *Adv. Energy Mater.* **2018**, *8*, 1801903. [CrossRef]
9. Castillo, M.S.; Liu, X.; Abd-AlHamid, F.; Connelly, K.; Wu, Y. Intelligent Windows for Electricity Generation: A Technologies Review. *Build. Simul.* **2022**, *15*, 1747–1773. [CrossRef]
10. Meinardi, F.; Bruni, F.; Brovelli, S. Luminescent Solar Concentrators for Building-Integrated Photovoltaics. *Nat. Rev. Mater.* **2017**, *2*, 17072. [CrossRef]
11. Yang, C.; Liu, D.; Renny, A.; Kuttipillai, P.S.; Lunt, R.R. Integration of Near-Infrared Harvesting Transparent Luminescent Solar Concentrators onto Arbitrary Surfaces. *J. Lumin.* **2019**, *210*, 239–246. [CrossRef]
12. Van Sark, W.G.J.H.M.; Barnham, K.W.J.; Slooff, L.H.; Chatten, A.J.; Büchtemann, A.; Meyer, A.; McCormack, S.J.; Koole, R.; Farrell, D.J.; Bose, R.; et al. Luminescent Solar Concentrators—A Review of Recent Results. *Opt. Express* **2008**, *16*, 21773. [CrossRef]
13. Li, Y.; Zhang, X.; Zhang, Y.; Dong, R.; Luscombe, C.K. Review on the Role of Polymers in Luminescent Solar Concentrators. *J. Polym. Sci. Part A Polym. Chem.* **2019**, *57*, 201–215. [CrossRef]
14. Rondão, R.; Frias, A.R.; Correia, S.F.H.; Fu, L.; de Zea Bermudez, V.; André, P.S.; Ferreira, R.A.S.; Carlos, L.D. High-Performance Near-Infrared Luminescent Solar Concentrators. *ACS Appl. Mater. Interfaces* **2017**, *9*, 12540–12546. [CrossRef] [PubMed]
15. Zhang, B.; Zhao, P.; Wilson, L.J.; Subbiah, J.; Yang, H.; Mulvaney, P.; Jones, D.J.; Ghiggino, K.P.; Wong, W.W.H. High-Performance Large-Area Luminescence Solar Concentrator Incorporating a Donor–Emitter Fluorophore System. *ACS Energy Lett.* **2019**, *4*, 1839–1844. [CrossRef]
16. Corsini, F.; Tatsi, E.; Colombo, A.; Dragonetti, C.; Botta, C.; Turri, S.; Griffini, G. Highly Emissive Fluorescent Silica-Based Core/Shell Nanoparticles for Efficient and Stable Luminescent Solar Concentrators. *Nano Energy* **2021**, *80*, 105551. [CrossRef]
17. Lyu, G.; Kendall, J.; Meazzini, I.; Preis, E.; Bayseç, S.; Scherf, U.; Clément, S.; Evans, R.C. Luminescent Solar Concentrators Based on Energy Transfer from an Aggregation-Induced Emitter Conjugated Polymer. *ACS Appl. Polym. Mater.* **2019**, *1*, 3039–3047. [CrossRef]
18. Correia, S.F.H.; De Zea Bermudez, V.; Ribeiro, S.J.L.; André, P.S.; Ferreira, R.A.S.; Carlos, L.D. Luminescent Solar Concentrators: Challenges for Lanthanide-Based Organic-Inorganic Hybrid Materials. *J. Mater. Chem. A* **2014**, *2*, 5580–5596. [CrossRef]

19. Nolasco, M.M.; Vaz, P.M.; Freitas, V.T.; Lima, P.P.; André, P.S.; Ferreira, R.A.S.; Vaz, P.D.; Ribeiro-Claro, P.; Carlos, L.D. Engineering Highly Efficient Eu(III)-Based Tri-Ureasil Hybrids toward Luminescent Solar Concentrators. *J. Mater. Chem. A* **2013**, *1*, 7339–7350. [CrossRef]
20. Wu, K.; Li, H.; Klimov, V.I. Tandem Luminescent Solar Concentrators Based on Engineered Quantum Dots. *Nat. Photonics* **2018**, *12*, 105–110. [CrossRef]
21. Sadeghi, S.; Bahmani Jalali, H.; Melikov, R.; Ganesh Kumar, B.; Mohammadi Aria, M.; Ow-Yang, C.W.; Nizamoglu, S. Stokes-Shift-Engineered Indium Phosphide Quantum Dots for Efficient Luminescent Solar Concentrators. *ACS Appl. Mater. Interfaces* **2018**, *10*, 12975–12982. [CrossRef] [PubMed]
22. Bergren, M.R.; Makarov, N.S.; Ramasamy, K.; Jackson, A.; Guglielmetti, R.; McDaniel, H. High-Performance $CuInS_2$ Quantum Dot Laminated Glass Luminescent Solar Concentrators for Windows. *ACS Energy Lett.* **2018**, *3*, 520–525. [CrossRef]
23. Gong, X.; Jiang, H.; Cao, M.; Rao, Z.; Zhao, X.; Vomiero, A. Eu-Doped ZnO Quantum Dots with Solid-State Fluorescence and Dual Emission for High-Performance Luminescent Solar Concentrators. *Mater. Chem. Front.* **2021**, *5*, 4746–4755. [CrossRef]
24. Selopal, G.S.; Mohammadnezhad, M.; Besteiro, L.V.; Cavuslar, O.; Liu, J.; Zhang, H.; Navarro-Pardo, F.; Liu, G.; Wang, M.; Durmusoglu, E.G.; et al. Synergistic Effect of Plasmonic Gold Nanoparticles Decorated Carbon Nanotubes in Quantum Dots/TiO_2 for Optoelectronic Devices. *Adv. Sci.* **2020**, *7*, 2001864. [CrossRef]
25. Cheng, Y.; Ding, L. Perovskite/Si Tandem Solar Cells: Fundamentals, Advances, Challenges, and Novel Applications. *SusMat* **2021**, *1*, 324–344. [CrossRef]
26. Wei, M.; de Arquer, F.P.G.; Walters, G.; Yang, Z.; Quan, L.N.; Kim, Y.; Sabatini, R.; Quintero-Bermudez, R.; Gao, L.; Fan, J.Z.; et al. Ultrafast Narrowband Exciton Routing within Layered Perovskite Nanoplatelets Enables Low-Loss Luminescent Solar Concentrators. *Nat. Energy* **2019**, *4*, 197–205. [CrossRef]
27. Wu, Y.; Zhan, Y.; Xin, W.; Cao, W.; Li, J.; Chen, M.; Jiang, X.; Wang, J.; Sun, Z. Highly Emissive Carbon Dots/Organosilicon Composites for Efficient and Stable Luminescent Solar Concentrators. *ACS Appl. Energy Mater.* **2022**, *5*, 1781–1792. [CrossRef]
28. Gong, X.; Zheng, S.; Zhao, X.; Vomiero, A. Engineering High-Emissive Silicon-Doped Carbon Nanodots towards Efficient Large-Area Luminescent Solar Concentrators. *Nano Energy* **2022**, *101*, 107617. [CrossRef]
29. Griffini, G.; Levi, M.; Turri, S. Novel High-Durability Luminescent Solar Concentrators Based on Fluoropolymer Coatings. *Prog. Org. Coatings* **2014**, *77*, 528–536. [CrossRef]
30. Griffini, G.; Brambilla, L.; Levi, M.; Del Zoppo, M.; Turri, S. Photo-Degradation of a Perylene-Based Organic Luminescent Solar Concentrator: Molecular Aspects and Device Implications. *Sol. Energy Mater. Sol. Cells* **2013**, *111*, 41–48. [CrossRef]
31. Tanaka, N.; Barashkov, N.; Heath, J.; Sisk, W.N. Photodegradation of Polymer-Dispersed Perylene Di-Imide Dyes. *Appl. Opt.* **2006**, *45*, 3846. [CrossRef] [PubMed]
32. Earp, A.A.; Rawling, T.; Franklin, J.B.; Smith, G.B. Perylene Dye Photodegradation Due to Ketones and Singlet Oxygen. *Dye. Pigment.* **2010**, *84*, 59–61. [CrossRef]
33. Krumer, Z.; Pera, S.J.; van Dijk-Moes, R.J.A.; Zhao, Y.; de Brouwer, A.F.P.; Groeneveld, E.; van Sark, W.G.J.H.M.; Schropp, R.E.I.; de Mello Donegá, C. Tackling Self-Absorption in Luminescent Solar Concentrators with Type-II Colloidal Quantum Dots. *Sol. Energy Mater. Sol. Cells* **2013**, *111*, 57–65. [CrossRef]
34. Mateen, F.; Lee, S.Y.; Hong, S.-K. Luminescent Solar Concentrators Based on Thermally Activated Delayed Fluorescence Dyes. *J. Mater. Chem. A* **2020**, *8*, 3708–3716. [CrossRef]
35. Xu, L.; Yao, Y.; Bronstein, N.D.; Li, L.; Alivisatos, A.P.; Nuzzo, R.G. Enhanced Photon Collection in Luminescent Solar Concentrators with Distributed Bragg Reflectors. *ACS Photonics* **2016**, *3*, 278–285. [CrossRef]
36. Huang, J.; Zhou, J.; Haraldsson, T.; Clemments, A.; Fujii, M.; Sugimoto, H.; Xu, B.; Sychugov, I. Triplex Glass Laminates with Silicon Quantum Dots for Luminescent Solar Concentrators. *Sol. RRL* **2020**, *4*, 2000195. [CrossRef]
37. Yang, C.; Zhang, J.; Peng, W.-T.; Sheng, W.; Liu, D.; Kuttipillai, P.S.; Young, M.; Donahue, M.R.; Levine, B.G.; Borhan, B.; et al. Impact of Stokes Shift on the Performance of Near-Infrared Harvesting Transparent Luminescent Solar Concentrators. *Sci. Rep.* **2018**, *8*, 16359. [CrossRef]
38. Corsini, F.; Nitti, A.; Tatsi, E.; Mattioli, G.; Botta, C.; Pasini, D.; Griffini, G. Large-Area Semi-Transparent Luminescent Solar Concentrators Based on Large Stokes Shift Aggregation-Induced Fluorinated Emitters Obtained Through a Sustainable Synthetic Approach. *Adv. Opt. Mater.* **2021**, *9*, 2100182. [CrossRef]
39. Banal, J.L.; White, J.M.; Ghiggino, K.P.; Wong, W.W.H. Concentrating Aggregation-Induced Fluorescence in Planar Waveguides: A Proof-of-Principle. *Sci. Rep.* **2015**, *4*, 4635. [CrossRef]
40. Delgado-Sanchez, J.-M. Luminescent Solar Concentrators: Photo-Stability Analysis and Long-Term Perspectives. *Sol. Energy Mater. Sol. Cells* **2019**, *202*, 110134. [CrossRef]
41. Mateen, F.; Hwang, T.G.; Boesel, L.F.; Choi, W.J.; Kim, J.P.; Gong, X.; Park, J.M.; Hong, S. Luminescent Solar Concentrator Utilizing Energy Transfer Paired Aggregation-induced Emissive Fluorophores. *Int. J. Energy Res.* **2021**, *45*, 17971–17981. [CrossRef]
42. Botta, C.; Betti, P.; Pasini, M. Organic Nanostructured Host–Guest Materials for Luminescent Solar Concentrators. *J. Mater. Chem. A* **2013**, *1*, 510–514. [CrossRef]
43. Cappelli, A.; Villafiorita-Monteleone, F.; Grisci, G.; Paolino, M.; Razzano, V.; Fabio, G.; Giuliani, G.; Donati, A.; Mendichi, R.; Boccia, A.C.; et al. Highly Emissive Supramolecular Assemblies Based on π-Stacked Polybenzofulvene Hosts and a Benzothiadiazole Guest. *J. Mater. Chem. C* **2014**, *2*, 7897–7905. [CrossRef]

44. Huber, S.; Ruiz, A.Z.; Li, H.; Patrinoiu, G.; Botta, C.; Calzaferri, G. Optical Spectroscopy of Inorganic–Organic Host–Guest Nanocrystals Organized as Oriented Monolayers. *Inorg. Chim. Acta* **2007**, *360*, 869–875. [CrossRef]
45. Viani, L.; Tolbod, L.P.; Jazdzyk, M.; Patrinoiu, G.; Cordella, F.; Mura, A.; Bongiovanni, G.; Botta, C.; Beljonne, D.; Cornil, J.; et al. Spatial Control of 3D Energy Transfer in Supramolecular Nanostructured Host−Guest Architectures. *J. Phys. Chem. B* **2009**, *113*, 10566–10570. [CrossRef]
46. Karnjkar, Y.S.; Dinde, R.M.; Dinde, N.M.; Bawankar, K.N.; Hinge, S.P.; Mohod, A.V.; Gogate, P.R. Degradation of Magenta Dye Using Different Approaches Based on Ultrasonic and Ultraviolet Irradiations: Comparison of Effectiveness and Effect of Additives for Intensification. *Ultrason. Sonochem.* **2015**, *27*, 117–124. [CrossRef]
47. Moura, J.C.V.P.; Oliveira-Campos, A.M.F.; Griffiths, J. The Effect of Additives on the Photostability of Dyed Polymers. *Dye. Pigment.* **1997**, *33*, 173–196. [CrossRef]
48. Moreau, J.; Giovanella, U.; Bombenger, J.P.; Porzio, W.; Vohra, V.; Spadacini, L.; Di Silvestro, G.; Barba, L.; Arrighetti, G.; Destri, S.; et al. Highly Emissive Nanostructured Thin Films of Organic Host-Guests for Energy Conversion. *ChemPhysChem* **2009**, *10*, 647–653. [CrossRef]
49. Kitamura, C.; Tanaka, S.; Yamashita, Y. Design of Narrow-Bandgap Polymers. Syntheses and Properties of Monomers and Polymers Containing Aromatic-Donor and *o*-Quinoid-Acceptor Units. *Chem. Mater.* **1996**, *8*, 570–578. [CrossRef]
50. Sonar, P.; Singh, S.P.; Leclère, P.; Surin, M.; Lazzaroni, R.; Lin, T.T.; Dodabalapur, A.; Sellinger, A. Synthesis, Characterization and Comparative Study of Thiophene-Benzothiadiazole Based Donor-Acceptor-Donor (D-A-D) Materials. *J. Mater. Chem.* **2009**, *19*, 3228–3237. [CrossRef]
51. Sonar, P.; Singh, S.P.; Sudhakar, S.; Dodabalapur, A.; Sellinger, A. High-Mobility Organic Thin Film Transistors Based on Benzothiadiazole- Sandwiched Dihexylquaterthiophenes. *Chem. Mater.* **2008**, *20*, 3184–3190. [CrossRef]
52. Lakowicz, J.R. *Principles of Fluorescence Spectroscopy*; Lakowicz, J.R., Ed.; Springer: Boston, MA, USA, 2006; ISBN 978-0-387-31278-1.
53. Hintz, H.; Egelhaaf, H.J.; Peisert, H.; Chassé, T. Photo-Oxidation and Ozonization of Poly(3-Hexylthiophene) Thin Films as Studied by UV/VIS and Photoelectron Spectroscopy. *Polym. Degrad. Stab.* **2010**, *95*, 818–825. [CrossRef]
54. Zhen, Y.; Wang, J.; Li, J.; Fu, M.; Fu, F.; Zhang, Y.; Feng, J. Enhanced Photocatalytic Degradation for Thiophene by Ag/α-MoO3 Heterojunction under Visible-Light Irradiation. *J. Mater. Sci. Mater. Electron.* **2018**, *29*, 3672–3681. [CrossRef]
55. Abdou, M.S.A.; Holdcroft, S. Mechanisms of Photodegradation of Poly(3-Alkylthiophenes) in Solution. *Macromolecules* **1993**, *26*, 2954–2962. [CrossRef]
56. Che, Y.; Niazi, M.R.; Izquierdo, R.; Perepichka, D.F. Mechanism of the Photodegradation of A-D-A Acceptors for Organic Photovoltaics. *Angew. Chem. Int. Ed.* **2021**, *60*, 24833–24837. [CrossRef] [PubMed]
57. Hermabessiere, L.; Dehaut, A.; Paul-Pont, I.; Lacroix, C.; Jezequel, R.; Soudant, P.; Duflos, G. Occurrence and Effects of Plastic Additives on Marine Environments and Organisms: A Review. *Chemosphere* **2017**, *182*, 781–793. [CrossRef]
58. Vohra, V.; Devaux, A.; Dieu, L.-Q.; Scavia, G.; Catellani, M.; Calzaferri, G.; Botta, C. Energy Transfer in Fluorescent Nanofibers Embedding Dye-Loaded Zeolite L Crystals. *Adv. Mater.* **2009**, *21*, 1146–1150. [CrossRef]
59. Calzaferri, G.; Huber, S.; Maas, H.; Minkowski, C. Host–Guest Antenna Materials. *Angew. Chem. Int. Ed.* **2003**, *42*, 3732–3758. [CrossRef]
60. Xu, X.; Chueh, C.-C.; Yang, Z.; Rajagopal, A.; Xu, J.; Jo, S.B.; Jen, A.K.Y. Ascorbic Acid as an Effective Antioxidant Additive to Enhance the Efficiency and Stability of Pb/Sn-Based Binary Perovskite Solar Cells. *Nano Energy* **2017**, *34*, 392–398. [CrossRef]

Disclaimer/Publisher's Note: The statements, opinions and data contained in all publications are solely those of the individual author(s) and contributor(s) and not of MDPI and/or the editor(s). MDPI and/or the editor(s) disclaim responsibility for any injury to people or property resulting from any ideas, methods, instructions or products referred to in the content.